AIRFOIL PRESSURE DISTRIBUTION TESTS AS AFFECTED BY TURBULENCE

A THESIS

Submitted in partial fulfillment
of the requirements for the Degree
of Master of Science in Aeronautical Engineering

by

Leo A. Geyer

Georgia School of Technology
Atlanta, Georgia
1941

AIRFOIL PRESSURE DISTRIBUTION TESTS AS

AFFECTED BY TURBULENCE

Approved

Date Approved by Chairman May 27th, 1941

ACKNOWLEDGMENTS

The author wishes to express his sincere appreciation to Professor Montgomery Knight who suggested the investigation and made many helpful suggestions and criticisms during its development.

TABLE OF CONTENTS

AIRFOIL PRESSURE DISTRIBUTION TESTS AS AFFECTED BY TURBULENCE

I. SUMMARY

An investigation was made to determine the effects of various degrees of turbulence in the initial airstream on the pressure distribution over a Clark Y airfoil. A range of turbulence factor from 1.6 to 3.0 was obtained by the use of various mesh screens. The turbulence factor was determined by the use of pressure sphere tests. The minimum test Reynolds Number was 150,000 and the maximum effective Reynolds Number 660,000.

The purpose of the tests was to determine: (1) the effect of turbulence on the pressure distribution, (2) the flow separation points on the airfoil surface, and (3) whether the use of effective Reynolds Number is justified in the range below 500,000.

It was found that the effects of various degrees of turbulence on the pressure distribution were relatively small and the determination of flow separation points was, therefore, only approximate. It appears that the use of effective Reynolds Number for maximum lift over the test range is justified.

II. INTRODUCTION

It has long been well known that the Reynolds Number has an important influence on airfoil characteristics. The extrapolation of wind tunnel test results to full-scale values were, until recently, made on the basis of this scale effect only. During the past few years it has become increasingly clear that aerodynamic characteristics are not simply connected by the single variable of scale, but that a new independent variable, termed "turbulence", has an effect which, under certain conditions, is of at least equal importance as the effects of Reynolds Number.

The word turbulence is used in a rather vague sense to mean any departure from steady flow. Specifically, turbulence connotes fluctuations with time, that is, the speed at any point in a flow fluctuates from instant to instant about a mean value.[1] The fluctuations are not periodic and their amplitude is generally small.

Turbulence, unlike Reynolds Number, is not readily defined in terms of physical quantities. It may be defined, however, by its effect on the characteristics of certain bodies. Prandtl in 1914 proposed the use of the sphere as an indicator of turbulence. By this method the value of the Reynolds Number of a sphere for a drag coefficient of 0.3 is determined, this being called the "critical"Reynolds Number. This critical Reynolds Number of a sphere is a measurement of the aerodynamic effect of the scale of turbulence on a particular body and is not a direct measurement of the turbulence. A direct measurement of the intensity of turbulence

---

[1] H.L. Dryden, "Turbulence, Companion of Reynolds Number," Journal of the Aeronautical Sciences, Vol. I, No.2, April, 1934, pp.67-75.

may be made by the use of the hot-wire anemometer.[2] Dryden[3] made a correlation between the intensity of turbulence as measured by a hot-wire anemometer and the critical Reynolds Numbers of spheres. The results show close agreement and the use of the sphere as a turbulence indicator was confirmed.

Since the measurement of sphere resistance to obtain critical Reynolds Number is somewhat inconvenient, Dryden in 1933 suggested the use of a "pressure sphere" as a turbulence indicator. This method consists of measuring the difference in pressure Δp between the front and rear portions of the sphere. If a pressure $\frac{\Delta p}{q}$ is plotted against values of the Reynolds Number based on the sphere diameter, a variation similar to the variation of the drag coefficient with Reynolds Number is found, thus permitting the approximate determination of critical Reynolds Number. A résumé of the theory of this method is given by Platt.[4] The pressure method, because of the ease and rapidity with which results could be obtained, was used in this series of tests to determine the critical Reynolds Number.

It appears that the effects of scale and turbulence on an airfoil

---

2 H. L. Dryden and A. M. Kuethe, Effect of Turbulence in Wind Tunnel Measurements, U.S. National Advisory Committee for Aeronautics, Technical Report No.342, 1929.

3 H. L. Dryden, G. B. Schubauer, W. C. Mock, Jr., and H. K. Skramstad, Measurements of Intensity and Scale of Wind-Tunnel Turbulence and Their Relation to the Critical Reynolds Number of Spheres, U. S. National Advisory Committee for Aeronautics, Technical Report No.581, 1937.

4 R. C. Platt, Turbulence Factors of N.A.C.A. Wind Tunnels as Determined by Sphere Tests, U. S. National Advisory Committee for Aeronautics, Technical Report No.558, 1936.

shape may be divided into two types as pointed out by Dryden.[5] First, the effective increase of viscosity due to turbulent mixing, and second, the effect of turbulence on the characteristics associated with the transition from laminar to turbulent flow in the boundary layer. The second effect is characterized by a sudden change between two types of flow, one resulting from separation of the laminar boundary layer, the other from delayed separation of the turbulent boundary layer. The results of this report depend upon the latter effect.

The exact nature of the occurrence of separation is not definitely known. Various explanations of this phenomenon are given in the literature.[6,7,8,9] No attempt will be made to review these explanations here, but all are in agreement with the following general aspects of the event.

The pressure distribution over the upper surface of a conventional airfoil section at lift coefficients in the neighborhood of the maximum is characterized by a low pressure point at a small distance from the

---

5 See footnote 3, p.3.

6 E. N. Jacobs, "Aerodynamics of Wing Sections for Airplanes," Society of Automotive Engineers Journal, Vol.34, No.3, March, 1934, pp.82-91.

7 E. Gruschwitz, The Process of Separation in the Turbulent Friction Layer, U. S. National Advisory Committee for Aeronautics, Technical Memorandums No.699, 1933.

8 C. B. Millikan and A. L. Klein, "The Effect of Turbulence," Aircraft Engineering, Vol.V, No.54, August, 1933, pp.169-174.

9 C. B. Millikan, "Further Experiments on the Variation of Maximum Lift Coefficient with Turbulence and Reynolds Number," A.S.M.E. Transactions, Vol.56, No.11, November, 1934, pp.815-825.

leading edge and by increasing pressures (positive pressure gradient) from this point in the direction of the trailing edge. Under these conditions the retarded air in the boundary layer may fail to progress against the positive pressure gradient. When this air fails to progress along the surface, it accumulates. The accumulating air produces separation of the flow, this separation, of course, reducing the lift.

Whether or not separation will develop is dependent on the resistance to separation of the boundary layer, the turbulent layer displaying much more resistance to separation than the laminar layer.

It has long been known that the transition from laminar to turbulent flow is hastened by the presence of initial turbulence in the air stream. The effect of this initial turbulence is much the same as the developed turbulence in that the separation of the boundary layer is still further delayed.

The associated scale effects that appear in a wind tunnel test in a turbulent stream tend to correspond with those that would appear in flight at a higher Reynolds Number. As pointed out by Dryden,[10] this led to the establishment of an approximate relationship between turbulence and Reynolds Number, that the effect of turbulence is equivalent to a shift in the Reynolds Number scale. The shifted Reynolds Number, which will be higher than the test Reynolds Number, is referred to as the "effective" Reynolds Number.

That this effective Reynolds Number can be obtained by multiplying the test Reynolds Number by a factor referred to as the

---

[10] H. L. Dryden, "Turbulence and the Boundary Layer," Journal of the Aeronautical Sciences, Vol.6, No.3, January, 1939, pp.85-100.

"turbulence factor"[11] has been pointed out by Jacobs. This turbulence factor is simply the critical Reynolds Number as obtained from the sphere tests divided into the critical Reynolds of spheres for free air (385,000).[12] An effective Reynolds Number is thus determined at which the tunnel results should be applied to flight conditions, or at which the results could be compared with those obtained in a different tunnel but corrected in a like manner for turbulence effect.

Von Kármán and Millikan[13] state that if two geometrically similar pressure distributions are compared, the boundary layer profiles at corresponding points are geometrically similar. This would mean that geometrically similar pressure distribution diagrams connote similar separation points of the boundary layer. It is known that the lift characteristics of an airfoil are determined by the boundary layer separation point.[14] Bicknell points out that for a given pressure distribution the transition point from laminar to turbulent flow is a function of Reynolds Number.

As was previously stated, turbulence in the initial airstream delays separation of the boundary layer and thus increases the lift

---

11 E. N. Jacobs and A. Sherman, Airfoil Section Characteristics as Affected by Variations of the Reynolds Number, U.S.National Advisory Committee for Aeronautics, Technical Report No.586, 1937.

12 Platt, op. cit.

13 T. von Kármán and C. B. Millikan, On the Theory of Laminar Boundary Layers Involving Separation, U.S.National Advisory Committee for Aeronautics, Technical Report No.504, 1934.

14 Joseph Bicknell, "The Correlation of Boundary Layer Transition Data," Journal of the Aeronautical Sciences, Vol.6,No.5, March, 1939, pp.203-205.

coefficient especially in the neighborhood of the stall. It was therefore proposed in planning the present test program to record the pressure distribution over an airfoil at various angles of attack in streams of different turbulence. These tests would be made at the same test Reynolds Number to eliminate the possibility of variation in the separation point due to this cause. It was hoped that any effect of the turbulence on the pressure distribution would be shown by the geometrically similar pressure diagrams obtained. The effect of the turbulence on the separation point would thus be shown.

Further study showed that it would be possible to check the use of effective Reynolds Number. If the conception of effective Reynolds Number is correct, then pressure diagrams taken at the same test Reynolds Number but under different degrees of turbulence should differ. To put it differently, if the pressure distribution was taken at the same effective Reynolds Number for different degrees of turbulence, the pressure diagrams should be geometrically similar.

III. APPARATUS

The experiments were carried out in the small wind tunnel of the Daniel Guggenheim School of Aeronautics at the Georgia School of Technology.[15] This tunnel has a square thirty inch jet and is of the Göttingen single-return type.

---

[15] G. A. Mahoff, L. B. Rumph, Jr., and W. R. Weems, Calibration of Small Wind Tunnel at Georgia Tech, Unpublished student technical report, Daniel Guggenheim School of Aeronautics, Georgia School of Technology, Report No.4, 1932-33.

In order to create varying degrees of turbulence three screens were placed individually across the upstream working section of the tunnel. These screens were of galvanized wire, being of standard make. A small portion of each of the screens, illustrating their relative size, is shown in Figures 1, 2, and 3. For the clear tunnel set-up, an empty frame replaced the screen in the same position.

The pressure sphere used to measure the turbulence was a standard five-inch black rubber bowling ball mounted on a tubular spindle (Figure 4). This was made similar to the spheres described by Platt.[16] Five holes, one at the front stagnation point and four equally spaced 22° from the downstream axis of the sphere, were equipped with pressure leads. Figure 5 shows the four static holes and the tubes at the end of the spindle for the pressure leads. These leads were connected to the total and static head outlets on a reservoir-type micromanometer so as to give the pressure differential Δp. The surface of the sphere was polished with wax to a mirror finish.

The sphere spindle fitted into a socket welded to the main support tube. This main support tube consisted of a five foot length of two inch pipe clamped to the top and bottom of the exit cone on the center line of the tunnel. Figure 6 shows the sphere in position. The side of the tunnel has been removed. The pressure lines were led outside the tunnel walls through the support tube.

Pressure distribution curves were made by means of a pressure wing of Clark Y section that completely spanned the closed jet. This wing was

---

[16] Platt, op. cit.

mounted in rotatable end plates which fitted in the walls of the tunnel on the horizontal center line and so located that the leading edge of the airfoil was eighteen inches downstream of the screen. The airfoil could be moved in a spanwise direction to change the position of the orifices with respect to the center line of the tunnel. The wing chord was six inches and the span fifty inches. Measurements of the angle of attack were made by placing an inclinometer on two pins set into one end of the wing. The rotatable end plates were locked at any desired angle by means of two clamps.

Figure 7 shows the pressure wing in place and the pressure distribution apparatus. Each orifice of the wing was connected to a tube of a multiple manometer which consisted of a bank of tubes mounted in a frame so that the angle of the tubes could be adjusted. Two tubes, one on each end of the manometer, were connected to a static pressure orifice located, as noted in Figure 7, in the tunnel wall at an angle of 45° up from the leading edge of the airfoil, upstream. The pressure measured by these two tubes was used as a reference.

Figure 8 shows the orifice positions on the profile of the airfoil (twice size). The tubes on the manometer were spaced to agree with the orifice positions, as shown in Figure 8, since the doubled scale facilitated the taking of the pressure diagrams.

Horizontal surveys of the jet were made at the airfoil location using a pitot tube of the Prandtl type. This was mounted on a clamp stand and was moved across the jet by sliding the stand along guides screwed to the floor, as shown in Figure 9.

IV. PROCEDURE

The procedure will be given for one tunnel condition. This same procedure was repeated for each screen and for the clear tunnel condition.

The dynamic pressure in the jet was determined by means of a micromanometer connected to a calibrated static pressure orifice in the high pressure section of the tunnel. The orifice calibration factor was determined by comparing the results of dynamic pressure readings using a pitot tube at the test section with the readings of the manometer connected to the static pressure orifice. Since the screen was installed downstream of the static pressure orifice, the static orifice reading was affected by the blocking effect of the screen and had to be calibrated for each screen.

A horizontal survey was made with the pitot tube to determine the velocity distribution across the jet. This was necessary in order to locate a point for uniform spanwise velocity distribution about the airfoil orifices in the pressure distribution runs. This point was found to occur about four inches to the left of the center line of the tunnel in all cases. The maximum variation in the velocity within six inches either side of the orifice position was found to be 2 per cent.

The pressure sphere was then set up in the tunnel. The static plate and the differential pressure between the impact hole and the wake holes were noted at various airspeeds. It was found that the differential pressure readings were definitely affected by temperature changes during the run. Therefore, a thermometer was inserted in the airstream and temperature recorded for each airspeed. In determining Reynolds Number

the density and viscosity were corrected by these temperature readings. A plot was then made of $\frac{\Delta p}{q}$ versus Reynolds Number and the critical Reynolds Number determined at $\frac{\Delta p}{q} = 1.22$. This determined the turbulence factor for reference.

The pressure airfoil was then mounted in the tunnel with the orifices located at the point where the velocity distribution was as uniform as possible. First, a run was made at a Reynolds Number based on the velocity at the critical Reynolds Number of the sphere and the chord of the airfoil, pressure distribution being recorded at measured angles of attack of $-6^{\circ}, -3^{\circ}, 0^{\circ}, 3^{\circ}, 6^{\circ}, 9^{\circ}, 12^{\circ}$, and 15°. Then a run was made at an airspeed of 80 feet per second, pressure distribution being recorded at measured angles of attack of $-6^{\circ}, 0^{\circ}, 9^{\circ}, 10.5^{\circ}$, and 15°. It was found that these angles gave the desired points.

In order to keep the pressure measurements as accurate as possible, it was necessary to obtain large deflections of the manometer liquids, which was accomplished by using two widely different specific gravities.

Liquid	Specific Gravity		
Alcohol	.813	at	22°C.
Carbon tetrachloride	1.59	at	22°C.

The proper choice of angle of the multiple manometer and of the liquid used gave pressure diagrams of approximately the same shape for the same angle of attack throughout the investigation.

To calculate the lift coefficient the area of the pressure diagrams was mechanically integrated. For a one inch strip of wing the pressure is in pounds per inch. If this pressure is multiplied by the chord, the normal force in pounds will result, which, divided by the dynamic pressure, q, gives the normal force coefficient C_N.

It was found that the reference static pressure as measured by the static orifice in the jet varied with change in angle of attack. This decrease in static pressure was due in part to the increase in velocity across the static orifice as a result of the increase in circulation about the airfoil as the angle of attack was increased. Since the angle of zero lift for a Clark Y airfoil is approximately -6°, at this angle of attack the circulation is negligible. Therefore, the difference between the atmospheric and the static pressure at -6° was used as a standard in each run, and the atmospheric pressures at higher angles of attack were corrected by this same increment. This correction brought the velocity heads at the various angles of attack into very close agreement.

V. RESULTS

Table I shows the results obtained from the pressure sphere tests, the actual curves being plotted in Figure 10 where $\frac{\Delta p}{q}$ is plotted against the Reynolds Number based on the sphere diameter. At the point where the differential pressure was equal to 1.22, the critical Reynolds Number of the sphere was noted. If the critical Reynolds Number of the sphere in free air (385,000) is divided by the critical Reynolds Number as noted in the tunnel, the turbulence factor is obtained.

Figures 11 and 12 show typical pressure distribution diagrams.

Figure 13 shows the normal force coefficients plotted against measured angle of attack for the runs made at the same test Reynolds Number of 220,000 under the various degrees of turbulence. Pressure drag coefficients were not determined since there were few orifices around the leading edge of the airfoil to give accurate pressure readings at this critical point.

Figures 14 and 15 show a superposition of the pressure distribution diagrams as obtained from the runs at the same test Reynolds Number of 220,000.

Figure 16 shows the normal force coefficients plotted against measured angle of attack as obtained from the runs made at a Reynolds Number based on the critical Reynolds Number of the sphere for each condition of turbulence. These Reynolds Numbers are given in Table II.

Figures 17 and 18 show a superposition of the pressure distribution diagrams as obtained from the runs made at critical Reynolds Number.

Figure 19 shows $C_{N_{max}}$ for each series of runs (one at the same test Reynolds Number and one at the same effective Reynolds Number) plotted against turbulence factor.

Figure 20 shows the angle of attack at $C_{N_{max}}$ for each series of runs plotted against the turbulence factor.

Figure 21 shows the values of $C_{N_{max}}$ as obtained from both series of runs plotted against Reynolds Number. The dashed curve was taken from Platt[17] representing values of $C_{L_{max}}$ for the Clark Y versus effective Reynolds Number.

VI. DISCUSSION

From the turbulence factors as obtained from Figure 10, it is shown that the mesh size does not necessarily determine the amount of turbulence but that the increased wire size for the large meshes seems to have the greatest effect in increasing the turbulence at the same distance

---

[17] Ibid.

downstream from the screen (as the sphere was located for all the runs).

In correcting the static pressure heads on the pressure distribution diagrams, the increment between the atmospheric pressure "A" and the tunnel static pressure "S" as measured at the angle of zero lift (-6°) was taken as a reference. In Figure 11 this increment is noted as the pressure difference. In Figure 12 this pressure difference was laid off above the atmospheric pressure and thus gave the corrected static pressure as noted.

In investigating the available data on the variation of the maximum lift coefficient with Reynolds Number for the Clark Y airfoil, the data best applicable for comparison with the results of this series of tests are given by Platt.[18] Platt shows values of $C_{L_{max}}$ as obtained from force tests plotted against effective Reynolds Number. These values were obtained from various tunnels and from full-scale tests under widely varying degrees of turbulence (turbulence factor = 1.1 to 5.83). A line faired through the reference points is practically horizontal from a Reynolds Number of 100,000 to 500,000 giving a constant $C_{L_{max}}$ of 1.22. This curve was replotted in Figure 21 and will be referred to later. From the above it is obvious that turbulence has practically no effect on the maximum lift of a Clark Y airfoil at low Reynolds Numbers. It immediately follows that the results obtained from the pressure distribution tests should show a similar characteristic.

Now referring to Figure 13 it is seen that turbulence has practically no effect on the values of C_N below the stall. But, in the neighborhood

---

[18] Ibid.

of the stall there is a definite variation in C_N under various degrees of turbulence. In attempting to explain this variation, the sources of error were carefully checked and duplicate runs made. The results of these check runs were practically indistinguishable from those shown. Error in measurement of angle of attack was ruled out by the close agreement of the curves up to 3 degrees angle of attack. The case of the lowest turbulence as obtained in the clear tunnel shows the greatest discrepancy. A feasible explanation of this could be due to the absence of a screen as a source of disturbance. It is known that screens create isotropic turbulence[19], that is turbulence in which the fluctuations have uniform velocity components in all directions. The turbulence existing in the clear tunnel may have been of such character as to cause the somewhat higher than normally expected lift coefficients for this particular case.

For the cases of higher turbulence the results seem to indicate a definite increase in lift coefficient with increase in turbulence. It is also to be noted that there is a slight shift of the angle of attack at $C_{N_{max}}$ which would indicate that the increased turbulence delays the reaching of the stall.

Figure 14 shows the variation in the pressure distribution at zero lift for the various degrees of turbulence. The variations shown are small and for this reason no conclusions as to the effect of turbulence on the distribution can be made. However, the definite "hump" occurring near the trailing edge on the upper surface is believed to be the result of turbulence. At this point it is seen that the lower degrees of turbulence

---

[19] See footnote 3, p.3.

give a higher negative pressure than the highest turbulence. The flow of lower turbulence tends to separate and thus creates a dead air space over the rear portion of the airfoil. The air flowing by this dead air space creates a negative pressure, much the same as the negative pressure created behind a sphere at Reynolds Number below the critical. However, the return of the flow to the surface is noted around the 95 per cent chord point where the high negative pressure is reduced. This "bubble" formed from the 80 per cent point to the 90 per cent point on the chord is reduced by the air of higher turbulence since it has enough energy to move along the surface (or closer to the surface) against the positive pressure gradient and thus limit the formation of the dead air region. Such a dead air region is often referred to as an indication of "pressure drag".[20]

Figure 15 shows the pressure distribution in the neighborhood of the stall. Variations in the similarity of the pressure diagrams are quite obvious and are due to the effects of turbulence. The higher negative pressures over the upper surface for the higher turbulence are a direct result of the ability of this flow to progress more rapidly against the positive pressure gradient. The pressures at the trailing edge are the result of the situation explained for Figure 6. The discrepancy in the maximum negative pressures at the leading edge is due to experimental error in reading the multiple manometer. At this point the pressure readings were quite difficult to make because of the wide fluctuations. Therefore, it was deemed impossible to draw any conclusions as to indications of leading edge separation from the pressure diagrams. While the

---

[20] See footnote 6, p.4.

pressures behind the 10 per cent of the chord seem to indicate such separation, the exact point where this begins cannot be diagnosed from the present results.

The results shown in Figure 16 are from the runs made for the purpose of investigating the use of effective Reynolds Number at low values of the Reynolds Number. While the effective Reynolds Number values are not identical (Table II), the variation is small enough to allow direct comparison of the results on the basis of effective Reynolds Number, the maximum deviation being 4 per cent. Since the whole conception of effective Reynolds Number is rather crude at best, this deviation was deemed unimportant.

The curve for the lowest degree of turbulence, i.e., for the clear tunnel, is again not in agreement with the other curves. This variation was previously discussed and an attempt made to account for it. The other curves show great similarity, especially in regard to the maximum lift occurring at practically the same angle of attack in each case. This would lead to the conclusion that the variation in test Reynolds Number in these runs creates sufficient scale effect to give these results.[21] Thus, in regard to angle of attack at maximum lift, effective Reynolds Number gives reasonable results.

The values of $C_{N_{max}}$ in these runs show variations with turbulence. However, the variation is much smaller in this case than that shown in Figure 6, being from 1.39 to 1.417 for the former and from 1.38 to 1.43 for the latter. This gives a percentage variation of 1.9 per cent for the

---

[21] See footnote 11, p.6.

runs at the same effective Reynolds Number as compared to 3.5 per cent for the runs at the same test Reynolds Number.

While it is difficult to doubt the data obtained in these two series of runs due to the many duplicate runs made, it may be assumed for the present that the runs at effective Reynolds Number lead to much more consistent results.

Figures 17 and 18 are obtained from the runs made at the same effective Reynolds Number. It can readily be seen that when compared with Figures 14 and 15, the variations in the pressure distribution are less for the runs at the same effective Reynolds Number than for runs at the same test Reynolds Number.

In Figure 19 arbitrary curves were drawn through the two sets of points as shown. It can be seen that the curve obtained for the run at the same effective Reynolds Number is horizontal which is in agreement with Platt.[22] The other curve indicates a definite increase in the maximum lift with increase in turbulence. This is more in agreement with the general results obtained from the pressure distribution tests.

Figure 20 shows similar characteristics of the effect of turbulence, there being little change in angle of attack at maximum lift for the runs at the same effective Reynolds Number and a definite increase of angle with increase of turbulence for the runs at the same test Reynolds Number.

Because of the scatter of points and the rather limited scope of the tests, it is difficult to make a definite statement concerning Figures 19 and 20. Indications are that the use of effective Reynolds Number at

---

[22] Platt, op. cit.

low Reynolds Number is worthwhile to attain better agreement in results. Referring now to Figure 21, all the $C_{N_{max}}$ values were plotted against Reynolds Number, both the test Reynolds Number and the effective Reynolds Number as noted. The curve drawn through the points shows excellent agreement with the reference curve. Of course, the discrepancy in the location of the two curves is because the $C_{N_{max}}$ curve from these tests is for an infinite aspect ratio while the $C_{L_{max}}$ reference curve was derived from force tests with finite aspect ratio. It will be seen that when the points for the runs at the same <u>test</u> Reynolds Number are plotted at <u>effective</u> Reynolds Number (test Reynolds Number times the turbulence factor) they seem to fall in much better agreement with the curve, the last two points indicating the general upturn of the curve around a Reynolds Number of 500,000 similar to the reference curve. This plot seems to give the best indication of the value of effective Reynolds Number. It is unfortunate that the characteristics of the Clark Y section are such that they are little affected by turbulence variations at low Reynolds Number. If time had permitted, these tests would have been extended to higher Reynolds Number where the variation is rather marked. This suggestion is made for future study.

VII. CONCLUSIONS

(1) The effects of various degrees of turbulence on the pressure distribution over an airfoil is relatively small at Reynolds Numbers below 500,000.

(2) At low Reynolds Number pressure distribution methods give only approximate location of the separation point because of the fluctuating nature of the air flow.

(3) The use of effective Reynolds Number for maximum lift appears to be justified at values below 500,000.

BIBLIOGRAPHY

Bicknell, Joseph, "The Correlation of Boundary Layer Transition Data," Journal of the Aeronautical Sciences, Vol.6, No.5, March, 1939, pp.203-205.

Dryden, H. L., "Turbulence and the Boundary Layer," Journal of the Aeronautical Sciences, Vol.6, No.3, January, 1939, pp.85-100.

_____, "Turbulence, Companion of Reynolds Number," Journal of the Aeronautical Sciences, Vol.1, No.2, April, 1934, pp.67-75.

_____, and A. M. Kuethe, Effect of Turbulence in Wind Tunnel Measurements, U.S.National Advisory Committee for Aeronautics, Technical Report No.342, 1929.

_____, G. B. Schubauer, W. C. Mock, Jr., and H. K. Skramstad, Measurements of Intensity and Scale of Wind-Tunnel Turbulence and Their Relation to the Critical Reynolds Number of Spheres, U.S. National Advisory Committee for Aeronautics, Technical Report No.581, 1937.

Gruschwitz, E., The Process of Separation in the Turbulent Friction Layer, U.S.National Advisory Committee for Aeronautics, Technical Memorandums No.699, 1933.

Jacobs, E. N., "Aerodynamics of Wing Sections for Airplanes," Society of Automotive Engineers Journal, Vol.34, No.3, March, 1934, pp. 82-91.

_____, and A. Sherman, Airfoil Section Characteristics as Affected by Variations of the Reynolds Number, U.S. National Advisory Committee for Aeronautics, Technical Report No.586, 1937.

Kármán, Theodore von and C. B. Millikan, On the Theory of Laminar Boundary Layers Involving Separation, U.S. National Advisory Committee for Aeronautics, Technical Report No. 504, 1934.

Mahoff, G. A., L. B. Rumph, and W. R. Weems, Calibration of Small Wind Tunnel at Georgia Tech. Unpublished student technical report, Daniel Guggenheim School of Aeronautics, Georgia School of Technology, Report No.4, 1932-33.

Millikan, C. B., "Further Experiments on the Variation of Maximum-Lift Coefficient with Turbulence and Reynolds Number," American Society of Mechanical Engineers Transactions, Vol.56, No.11, November, 1934, pp.815-825

_____, and A. L. Klein, "The Effect of Turbulence," Aircraft Engineering, Vol. V, No.54, August, 1933, pp.169-174.

Platt, R. C., Turbulence Factors of N.A.C.A. Wind Tunnels as Determined by Sphere Tests, U.S. National Advisory Committee for Aeronautics, Technical Report No.558, 1936.

TABLE I

Tunnel Condition	Critical Reynolds Number[1]	Turbulence Factor
Clear Tunnel	240,200	1.60
1/4" Screen	172,000	2.24
1/2" Screen	156,200	2.46
3/4" Screen	128,000	3.00

[1] Based on sphere diameter

TABLE II

Tunnel Condition	Test R. N.[2]	Turbulence Factor	Effective R.N.
Clear Tunnel	276,000	1.60	441,000
1/4" Screen	195,000	2.24	437,000
1/2" Screen	186,700	2.46	459,000
3/4" Screen	150,200	3.00	450,600

[2] Based on Airfoil Chord and Velocity Determined from Critical Reynolds Number of Spheres (Table I).

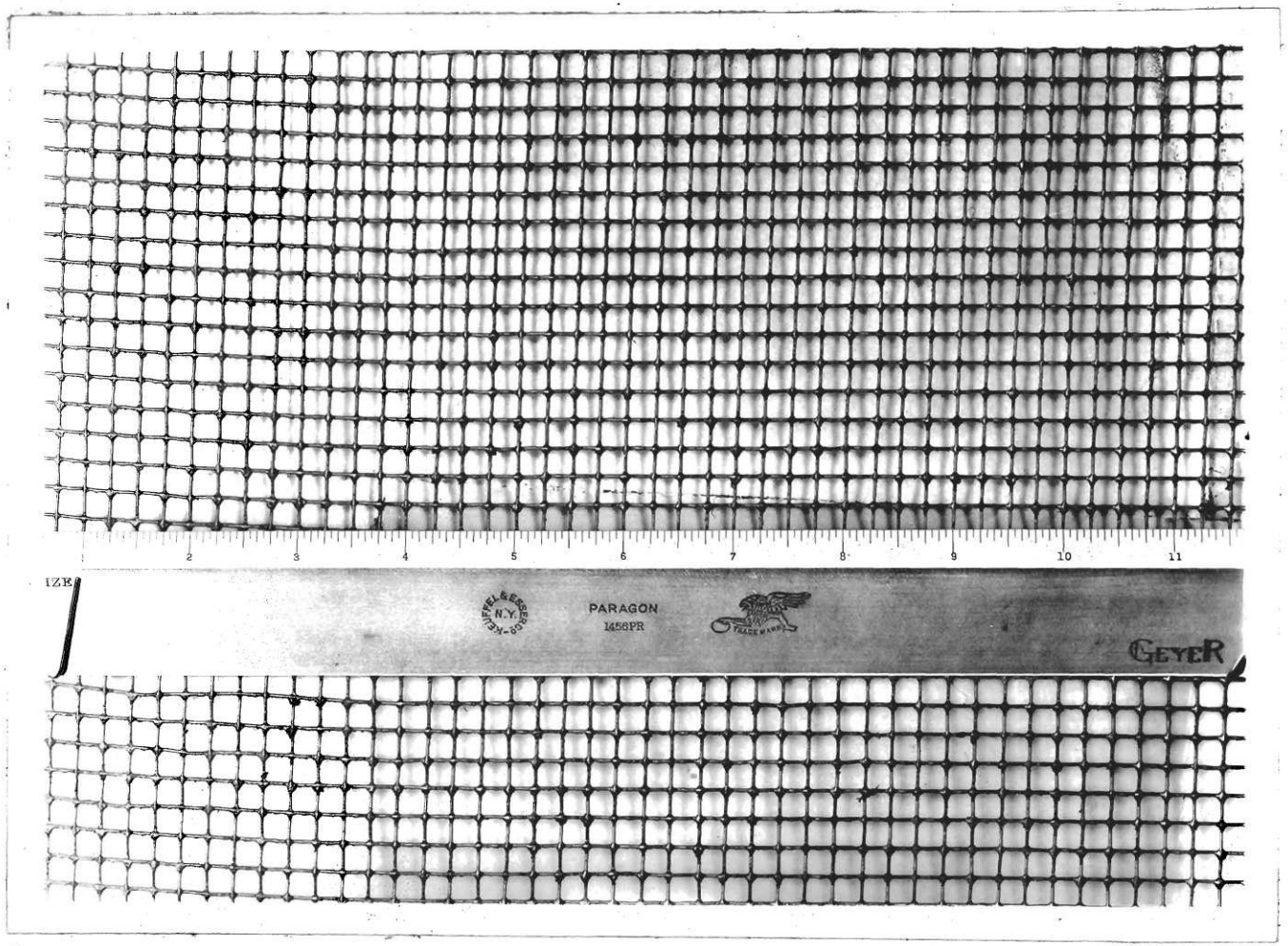

Fig. 1 Section of 1/4" Screen Used to Produce Initial Turbulence in Tunnel.

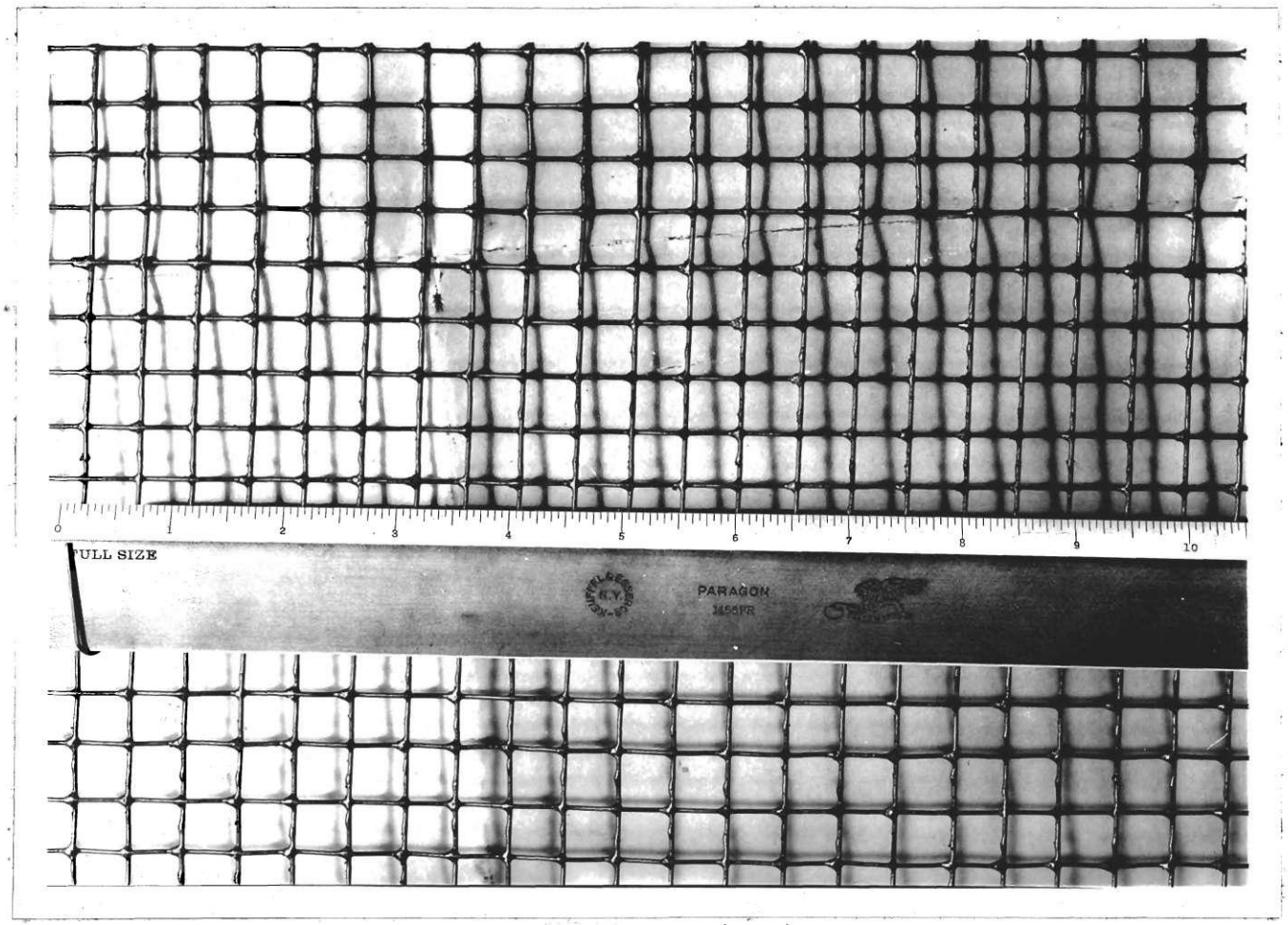

Fig. 2 Section of 1/2" Screen Used to Produce Initial Turbulence in Tunnel.

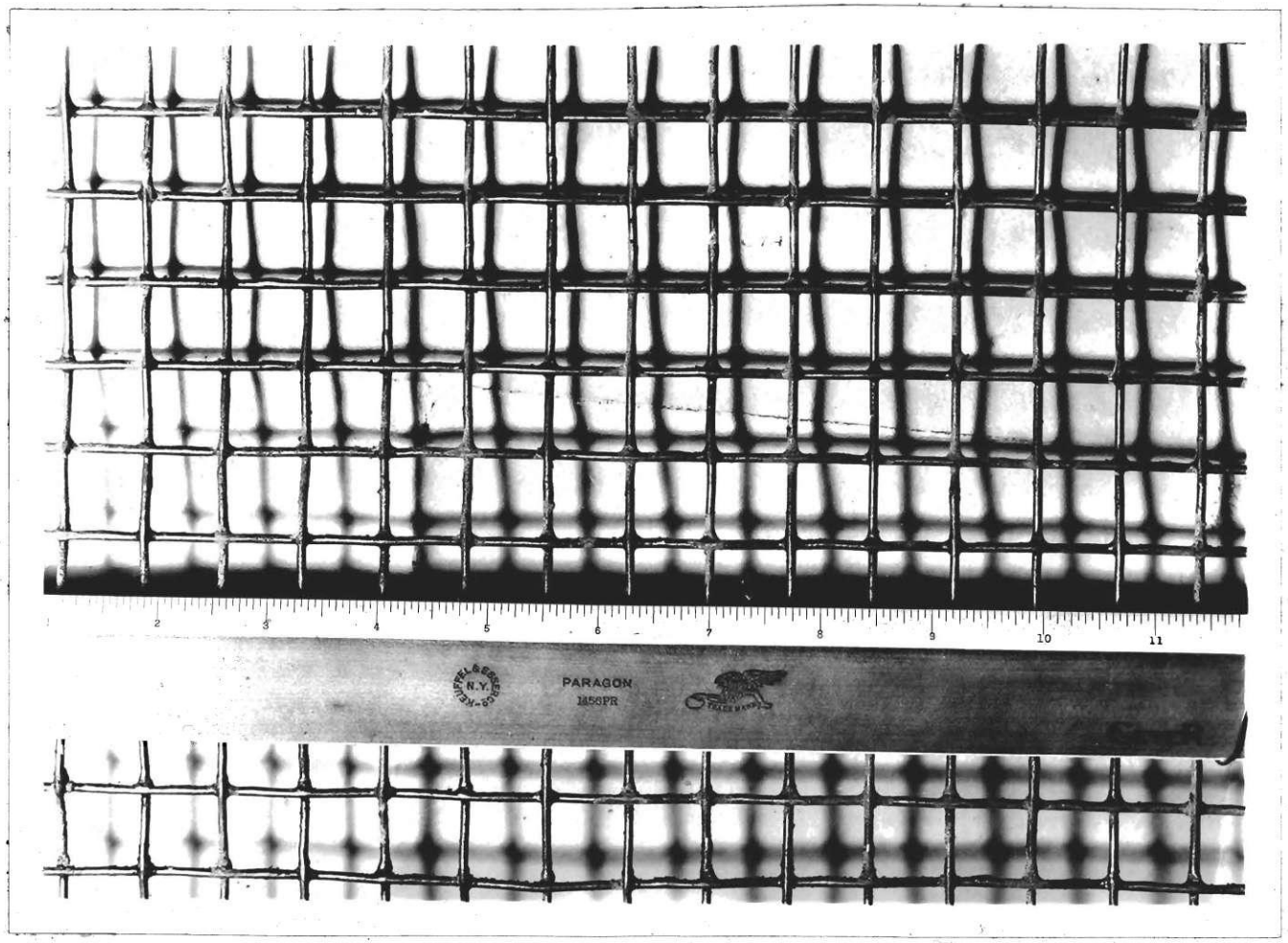

Fig. 3 Section of 3/4" Screen Used to Produce Initial Turbulence in Tunnel.

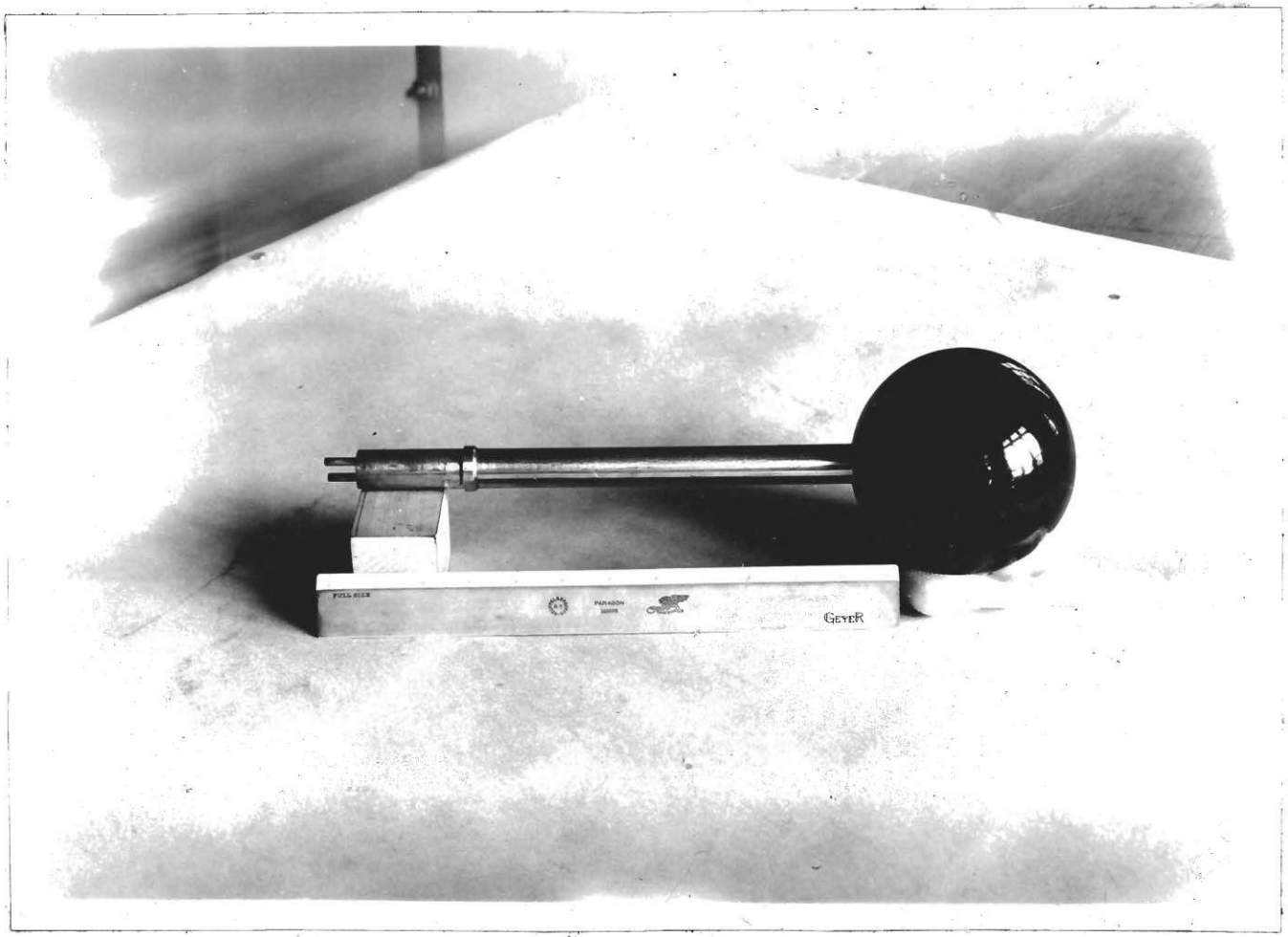

Fig. 4 Side View of Pressure Sphere.

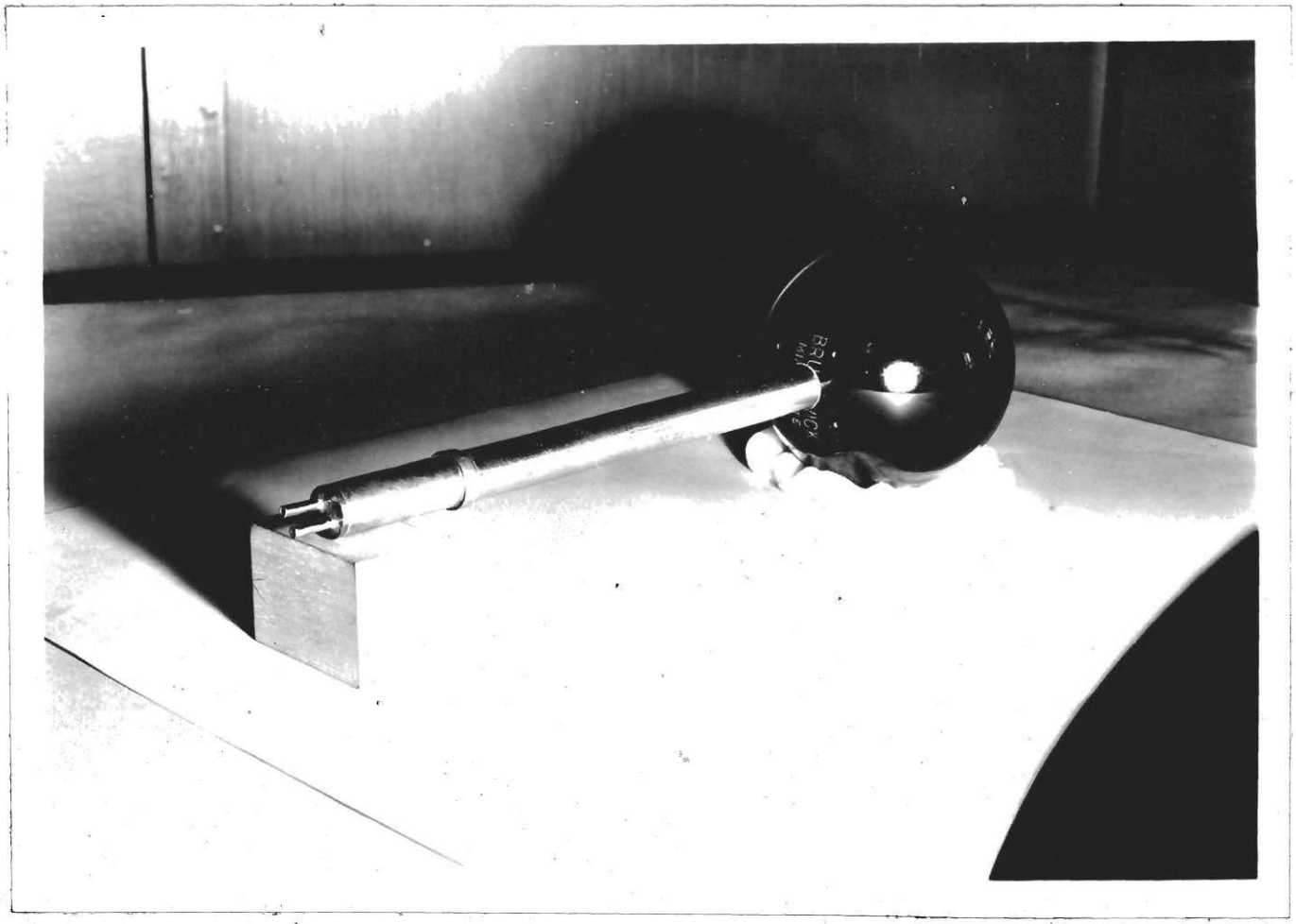

Fig. 5 Rear View of Pressure Sphere Showing Position of Rear Static-Pressure Holes and Pressure Leads at End of Spindle.

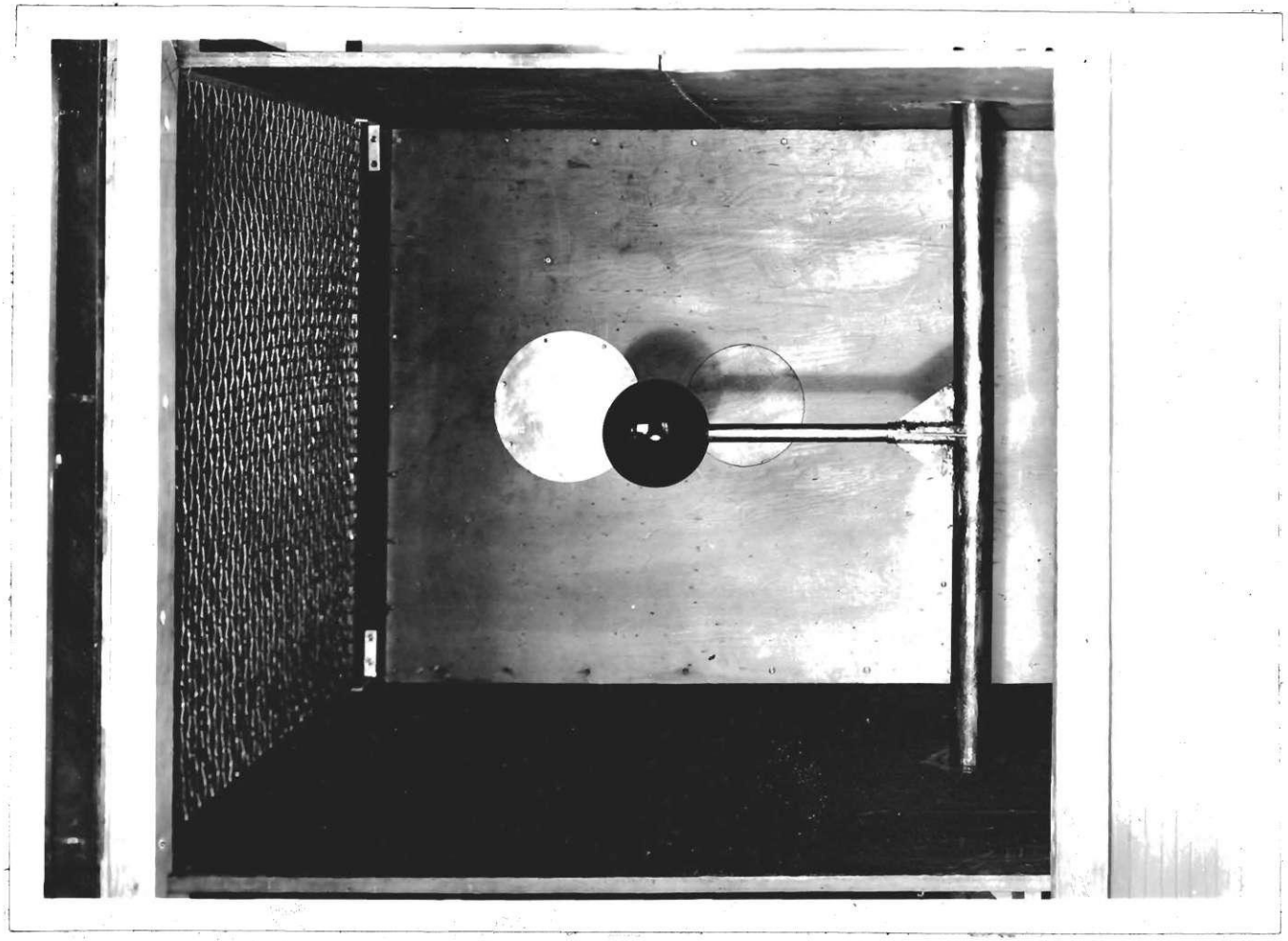

Fig. 6 View Showing Interior of Tunnel at Working Section with Pressure Sphere and 3/4" Screen in Place. Side Wall Has Been Removed.

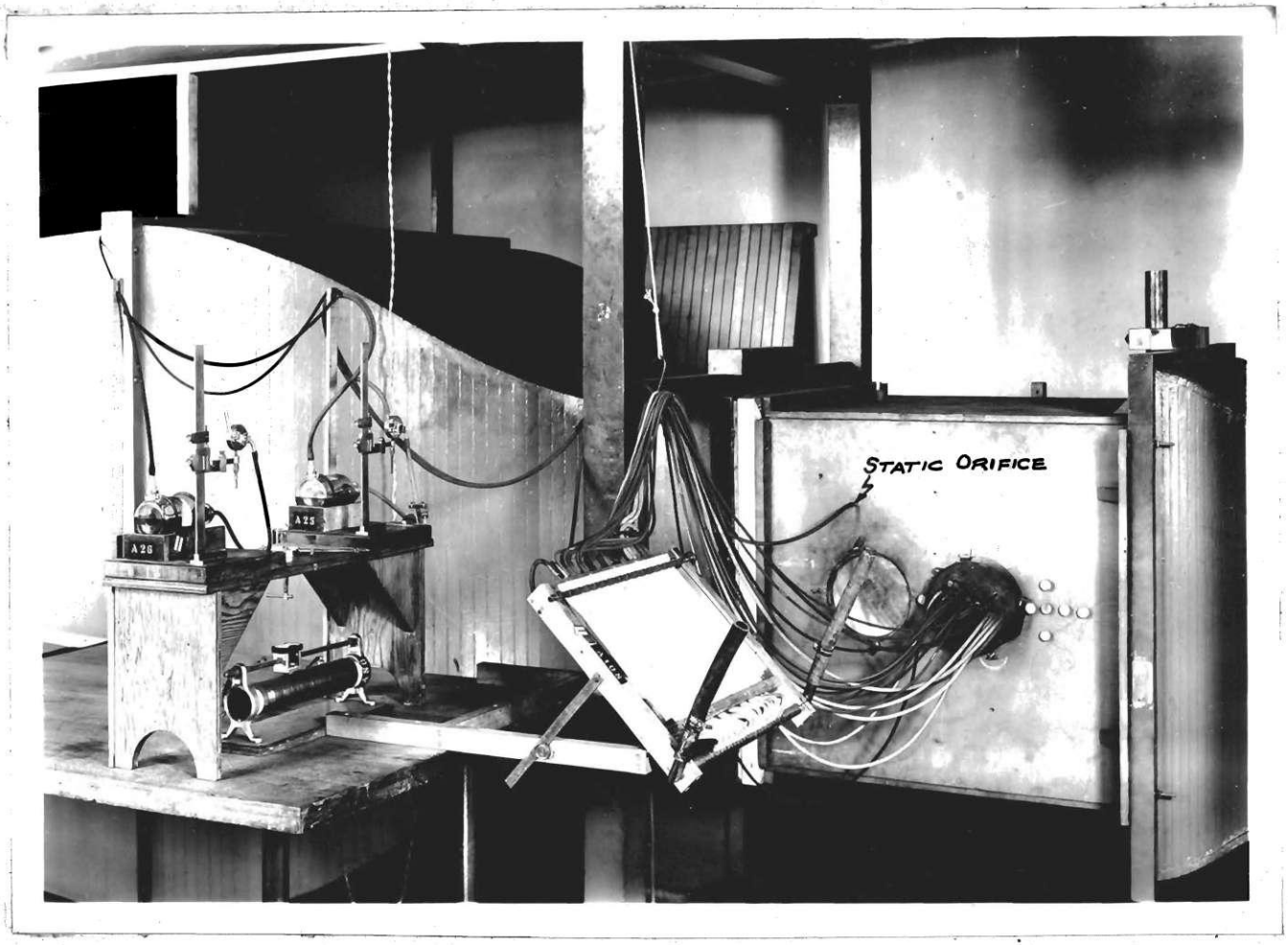

Fig. 7 View Showing Pressure Airfoil in Place and Rack Manometer Used to Obtain Pressure Distribution Diagrams.

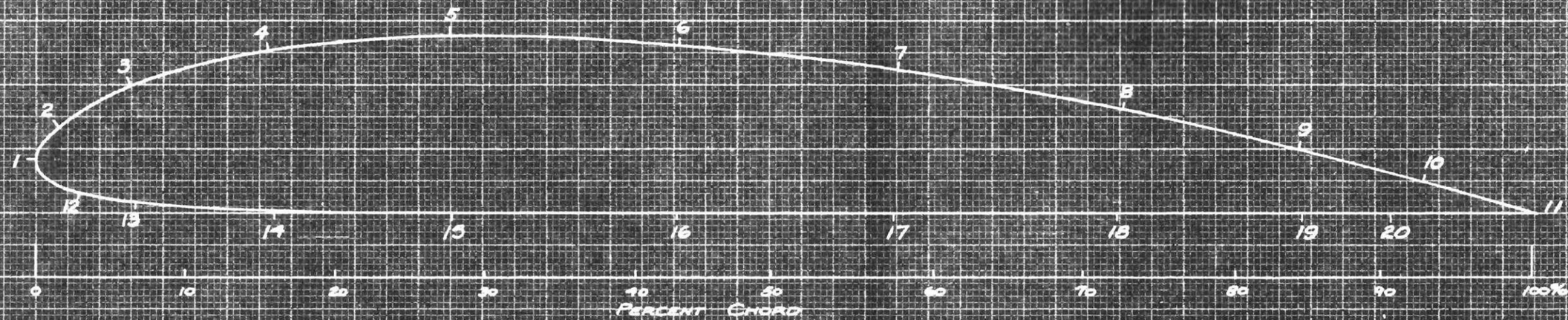

FIG. 8

LOCATION OF PRESSURE ORIFICES
ON PROFILE OF CLARK-Y

SCALE: 2"=1'

FOR DIMENSIONS SEE DRWG. #AE 39

DGSA GA. TECH.

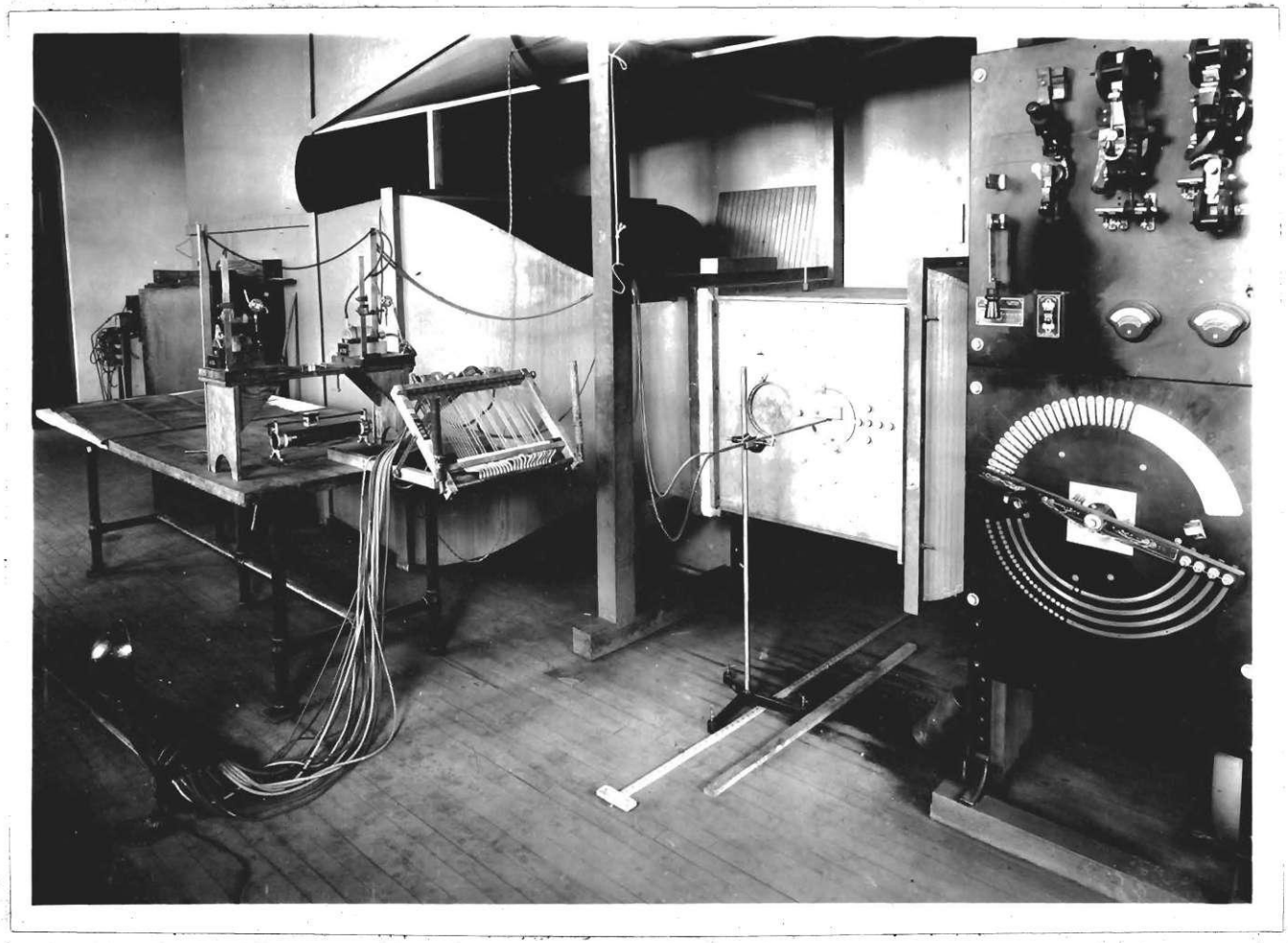

Fig. 9 General View of Apparatus Showing Pitot Tube in Place.

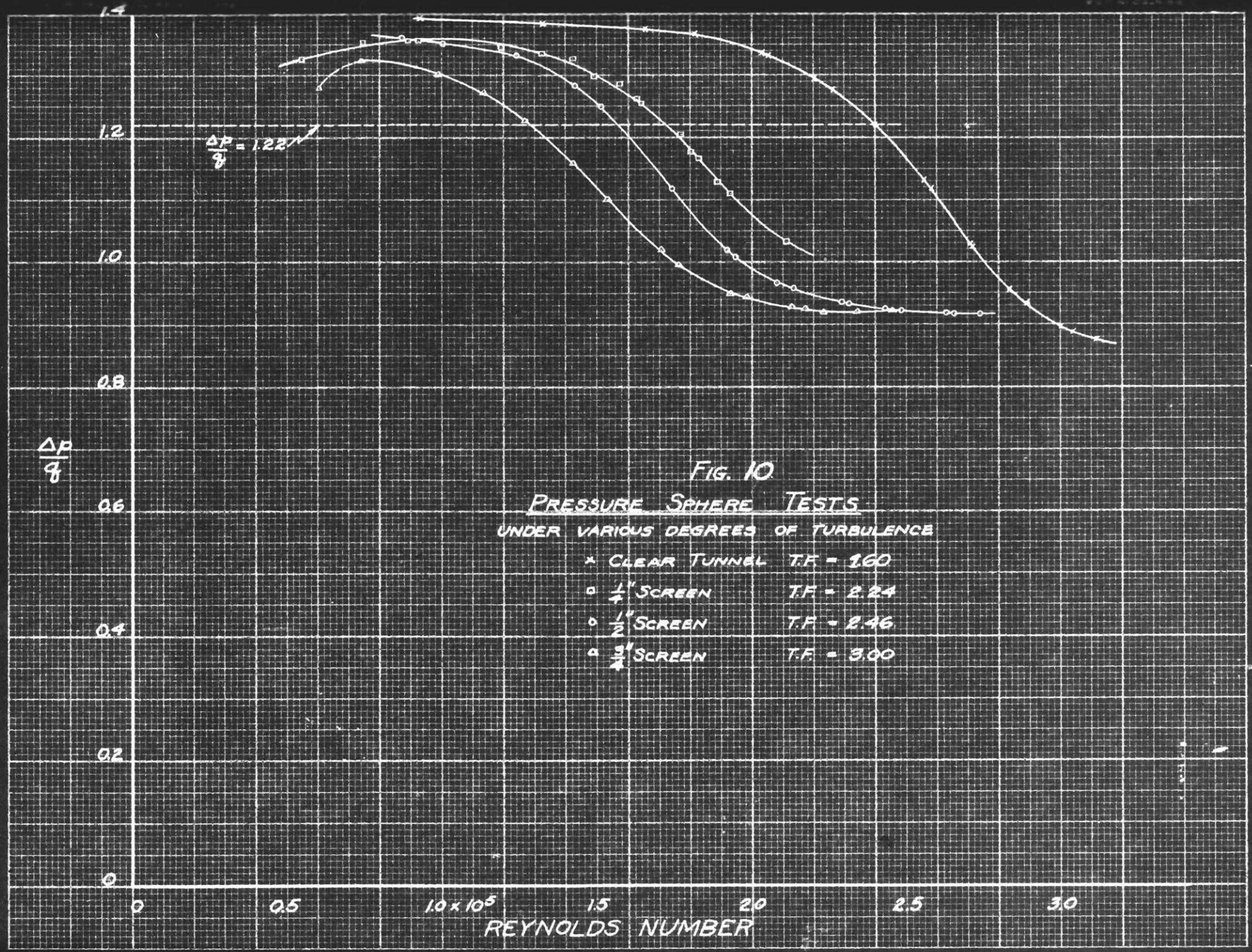

FIG. 10

PRESSURE SPHERE TESTS

UNDER VARIOUS DEGREES OF TURBULENCE

* CLEAR TUNNEL T.F = 1.60

□ $\frac{1}{4}$" SCREEN T.F = 2.24

○ $\frac{1}{2}$" SCREEN T.F = 2.46

△ $\frac{3}{4}$" SCREEN T.F = 3.00

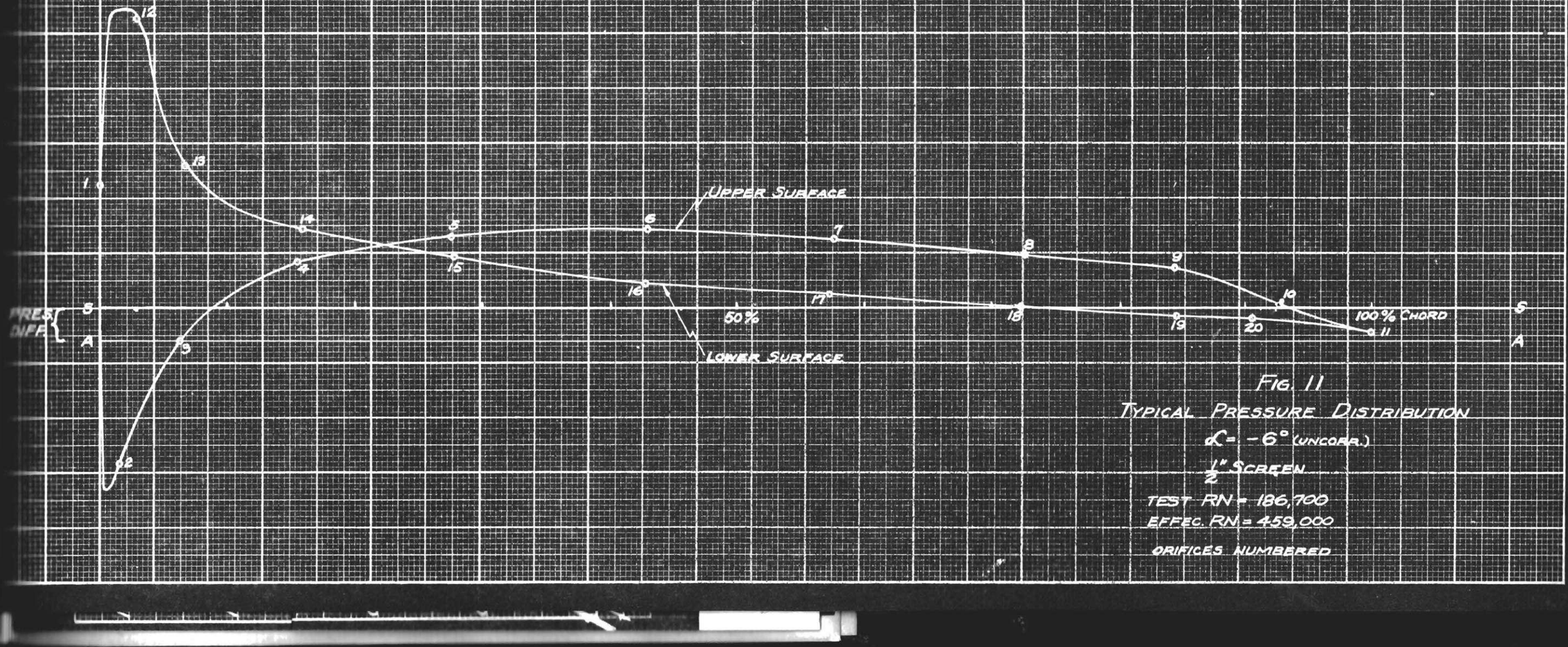

FIG. 11

TYPICAL PRESSURE DISTRIBUTION

$\alpha = -6°$ (UNCORR.)

$\frac{1}{2}$" SCREEN

TEST RN = 186,700

EFFEC. RN = 459,000

ORIFICES NUMBERED

UPPER SURFACE

PRES. DIFF. S A

CORRECTED STATIC PRESSURE

50%

100% CHORD S A

LOWER SURFACE

FIG. 12

TYPICAL PRESSURE DISTRIBUTION

α = 12° (UNCORR.)

$\frac{1}{2}$" SCREEN

TEST RN = 186,700

EFFEC. RN = 459,000

C_N - Normal Force Coefficient

1.4
1.3
1.2
1.1
1.0
0.9
0.8
0.7
0.6
0.5
0.4
0.3
0.2
0.1

-3 0 3 6 9 12

α - Angle of Attack in Degrees

FIG. 13

NORMAL FORCE COEFFICIENT
VS.
ANGLE OF ATTACK
(UNCORRECTED)

CONSTANT TEST RN = 220,000

×	CLEAR TUNNEL	EFFECTIVE RN = 332,000
△	1/4" SCREEN	" " = 493,000
○	1/2" SCREEN	" " = 541,000
□	3/4" SCREEN	" " = 660,000

KEUFFEL & ESSER CO. N. Y.

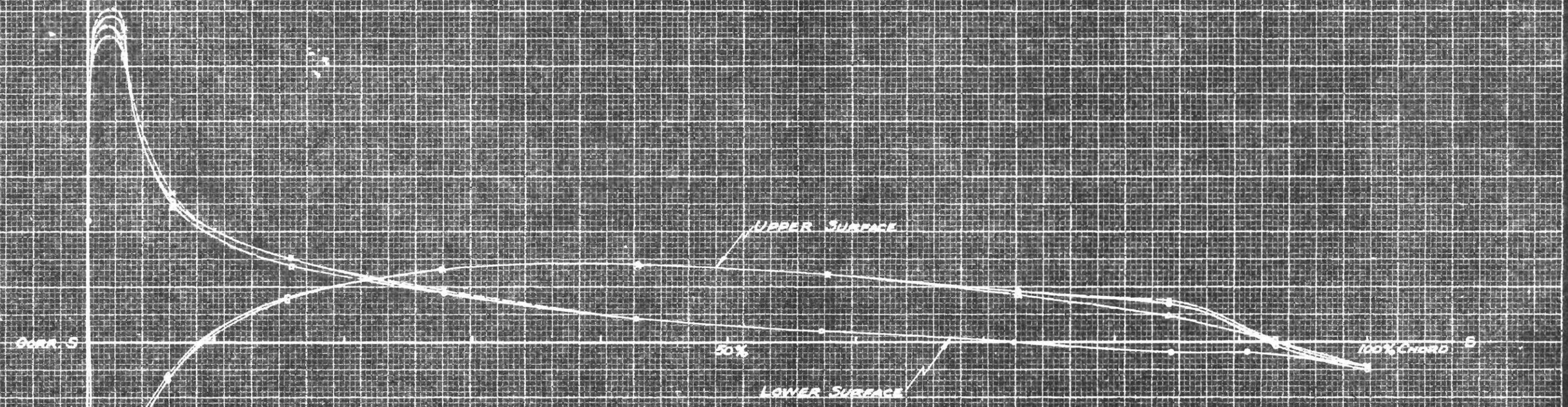

FIG. 14

SUPERPOSITION OF PRESSURE DISTRIBUTIONS

$\alpha = -6°$ (UNCORR.)

CONSTANT TEST RN = 220,000

□	CLEAR TUNNEL	EFFEC. RN =	352,000
○	1/4" SCREEN	" " =	493,000
×	1/2" SCREEN	" " =	541,000
△	3/4" SCREEN	" " =	660,000

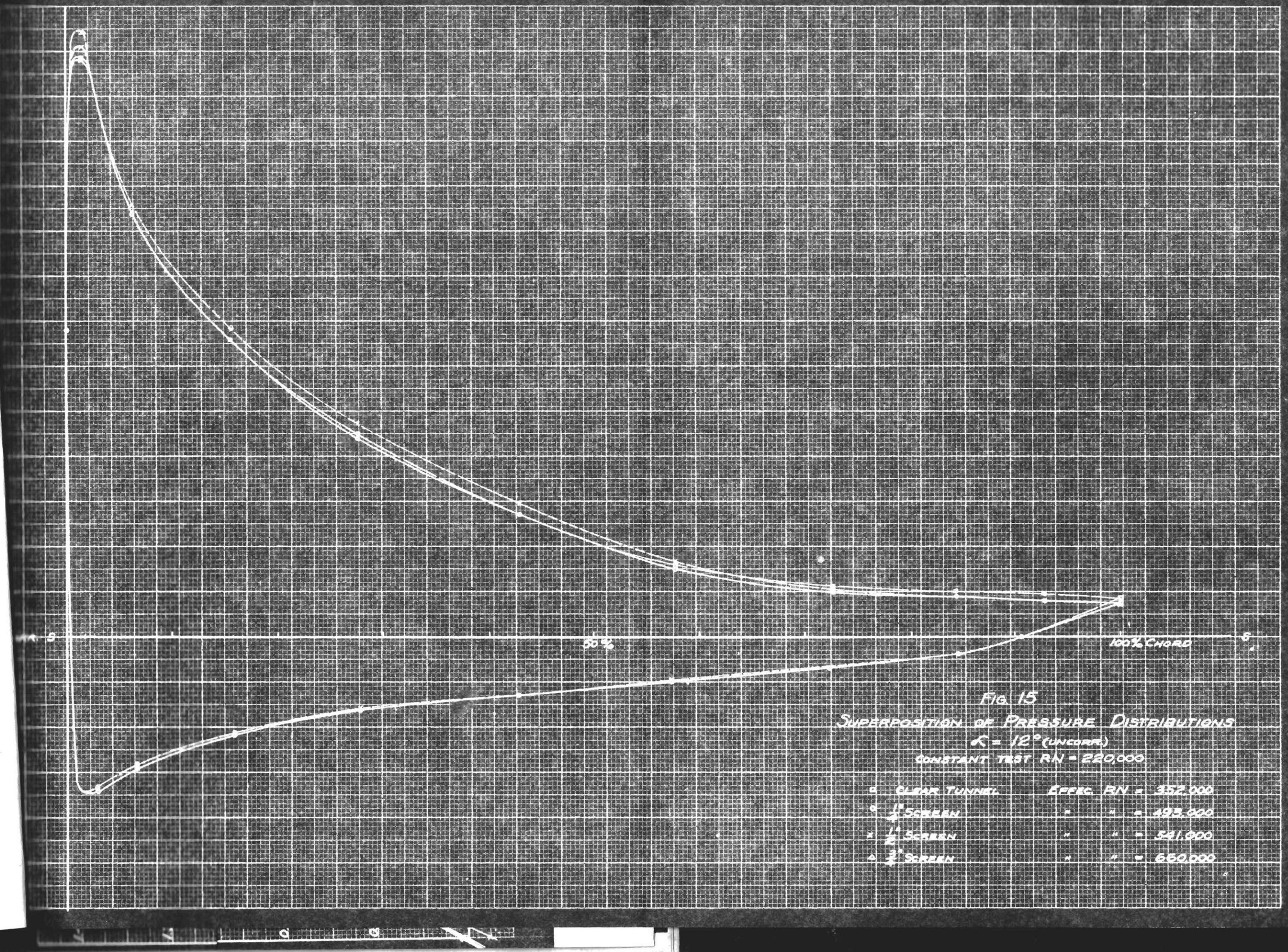

FIG. 15

SUPERPOSITION OF PRESSURE DISTRIBUTIONS

α = 12° (UNCORR.)

CONSTANT TEST RN = 220,000

○	CLEAR TUNNEL	EFFEC. RN =	352,000
□	½" SCREEN	" " =	493,000
×	¾" SCREEN	" " =	541,000
△	1" SCREEN	" " =	650,000

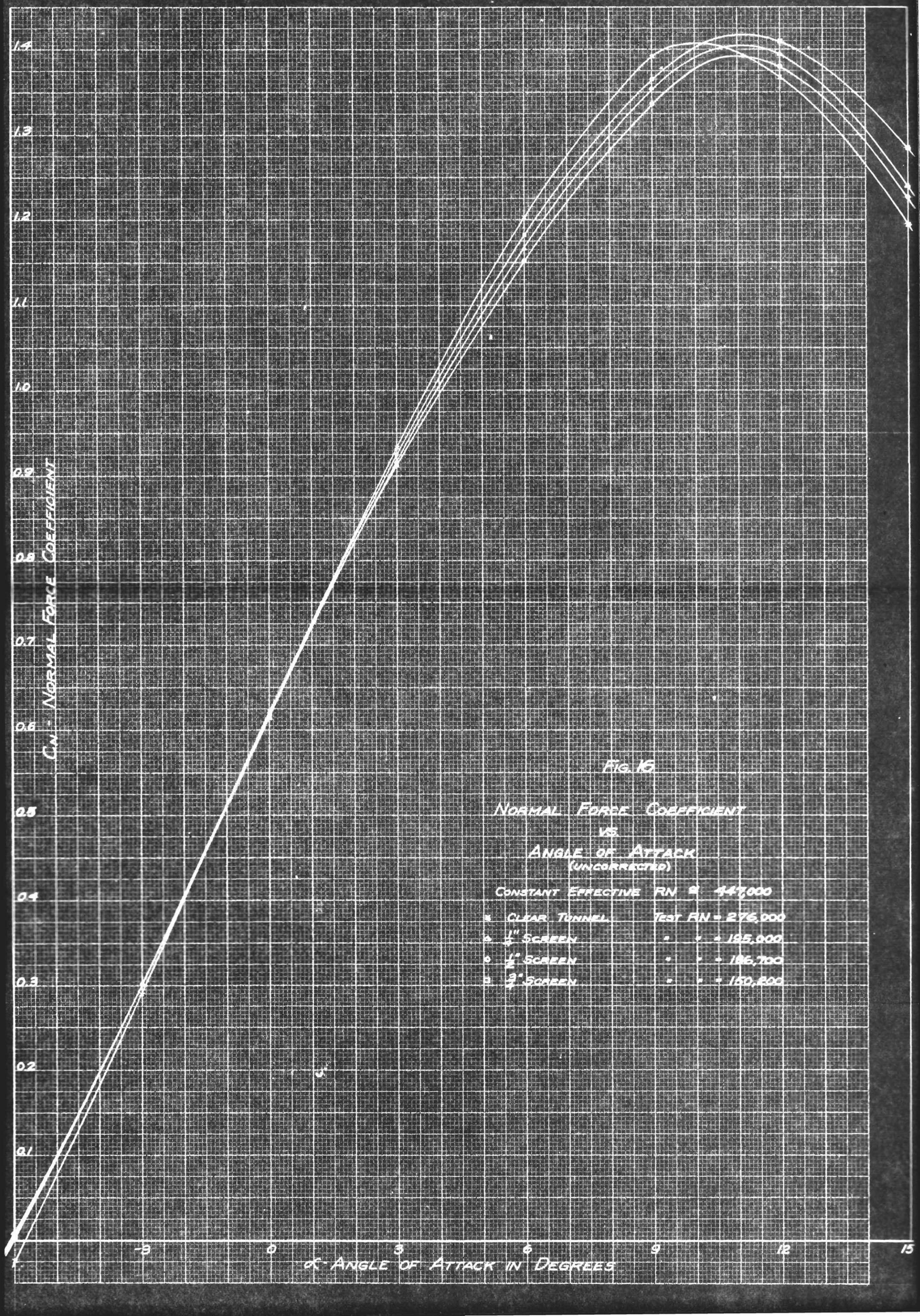

FIG. 16

NORMAL FORCE COEFFICIENT
VS.
ANGLE OF ATTACK
(UNCORRECTED)

CONSTANT EFFECTIVE RN @ 447,000

⊗	CLEAR TUNNEL	TEST RN = 276,000
⊙	1" SCREEN	" " = 195,000
○	½" SCREEN	" " = 186,700
⊙	¾" SCREEN	" " = 150,200

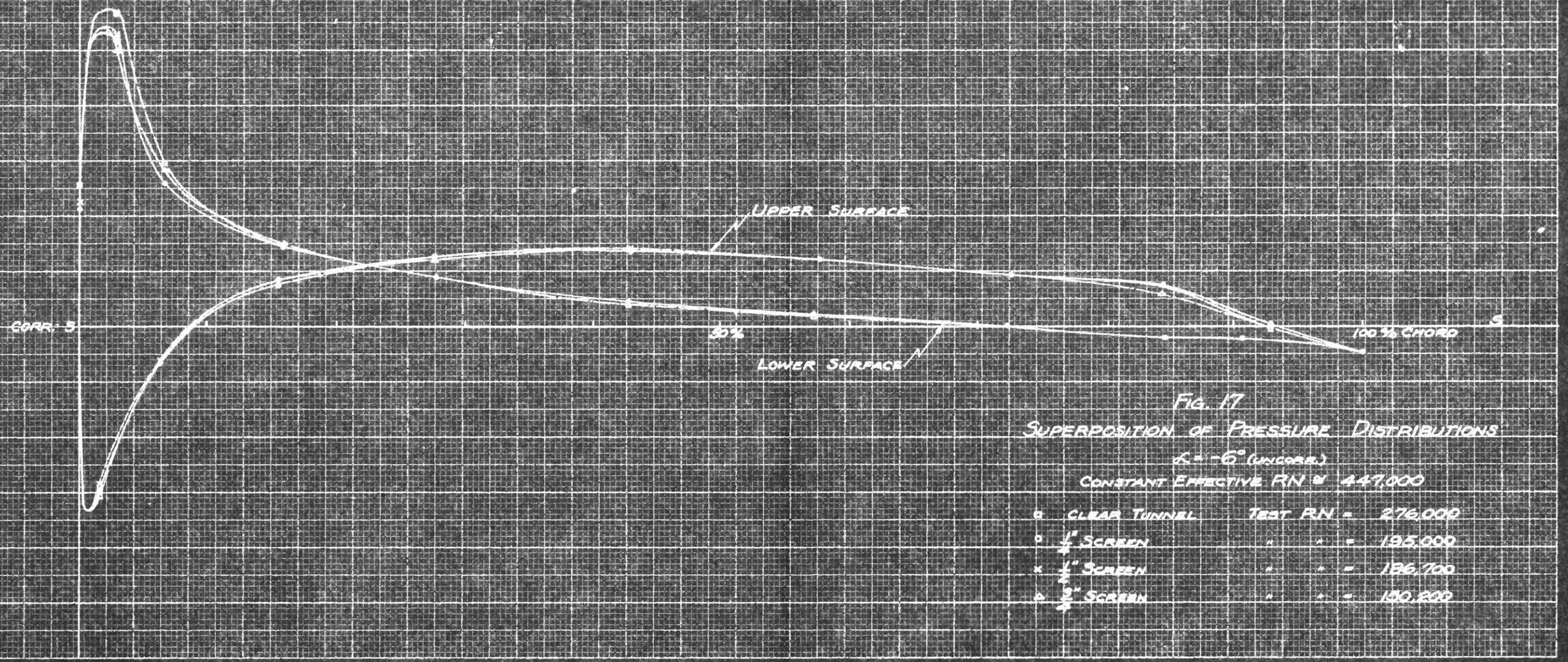

FIG. 17

SUPERPOSITION OF PRESSURE DISTRIBUTIONS

$\alpha = -6°$ (UNCORR.)

CONSTANT EFFECTIVE RN @ 447,000

□	CLEAR TUNNEL	TEST RN = 276,000
○	1/4" SCREEN	" " = 195,000
×	1/2" SCREEN	" " = 186,700
△	3/4" SCREEN	" " = 150,200

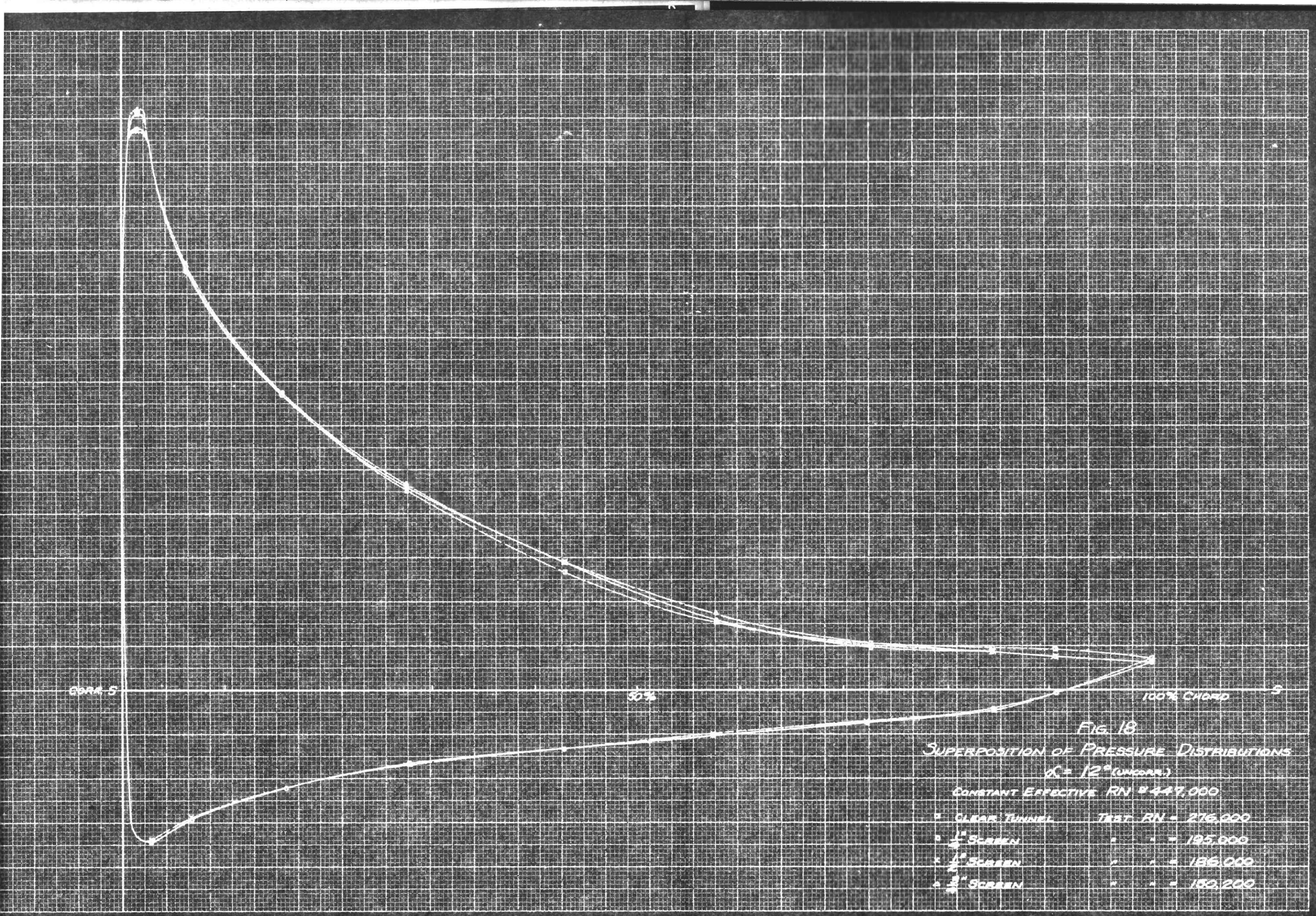

FIG. 18.

SUPERPOSITION OF PRESSURE DISTRIBUTIONS

$\alpha = 12°$ (UNCORR.)

CONSTANT EFFECTIVE RN = 447,000

a	CLOSED TUNNEL	TEST RN = 276,000
b	$\frac{1}{4}$" SCREEN	" " = 195,000
c	$\frac{1}{2}$" SCREEN	" " = 186,000
d	$\frac{3}{4}$" SCREEN	" " = 180,200

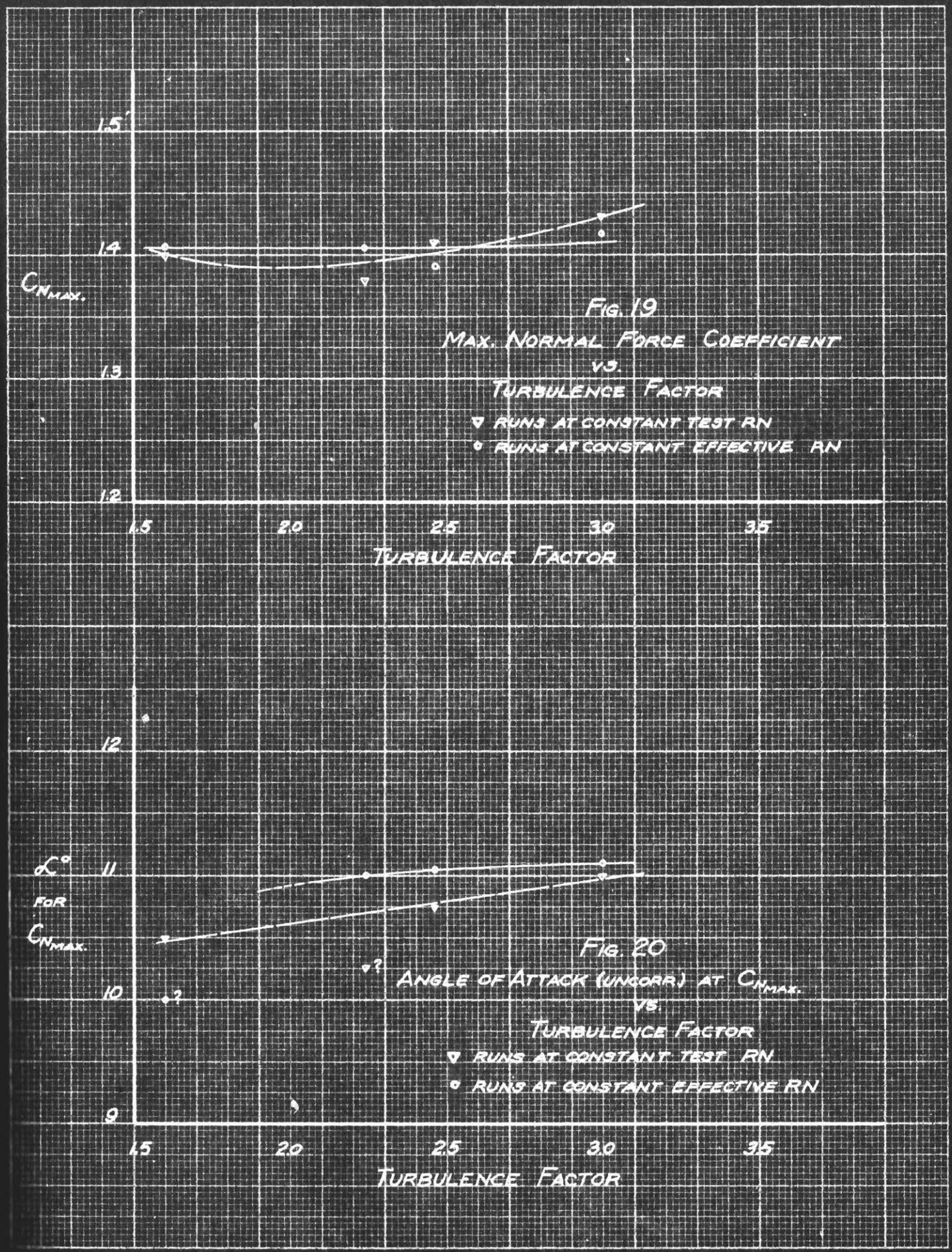
1.5
1.4
$C_{N_{MAX.}}$
1.3
1.2
1.5
2.0
2.5
3.0
3.5
TURBULENCE FACTOR
FIG. 19
MAX. NORMAL FORCE COEFFICIENT
VS.
TURBULENCE FACTOR
▽ RUNS AT CONSTANT TEST RN
○ RUNS AT CONSTANT EFFECTIVE RN
12
α° FOR $C_{N_{MAX.}}$
11
10
9
1.5
2.0
2.5
3.0
3.5
TURBULENCE FACTOR
FIG. 20
ANGLE OF ATTACK (UNCORR.) AT $C_{N_{MAX.}}$
VS.
TURBULENCE FACTOR
▽ RUNS AT CONSTANT TEST RN
○ RUNS AT CONSTANT EFFECTIVE RN

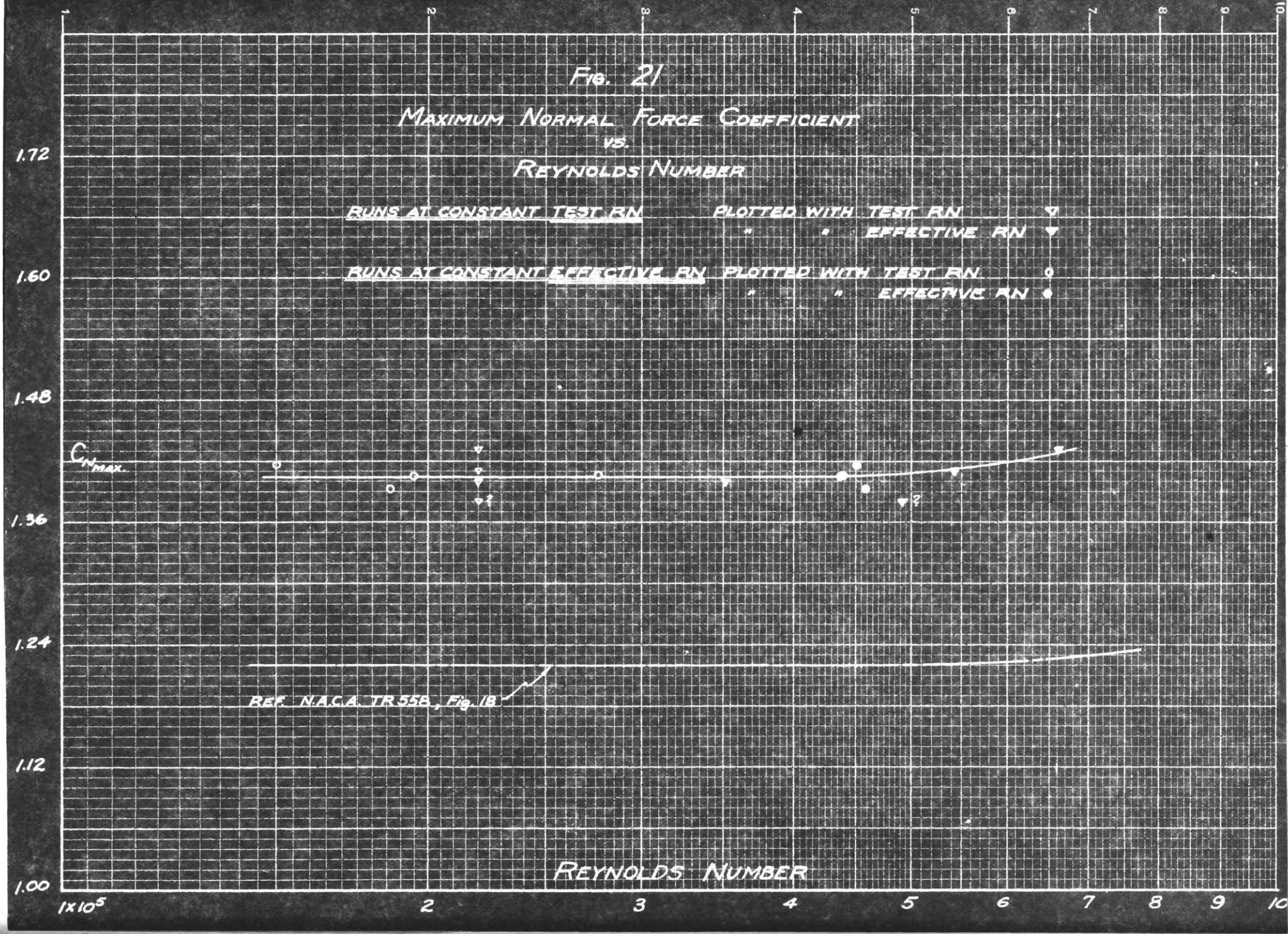
FIG. 21
MAXIMUM NORMAL FORCE COEFFICIENT
VS.
REYNOLDS NUMBER
RUNS AT CONSTANT TEST RN PLOTTED WITH TEST RN
" " EFFECTIVE RN
RUNS AT CONSTANT EFFECTIVE RN PLOTTED WITH TEST RN
" " EFFECTIVE RN
$C_{N_{MAX.}}$
1.72
1.60
1.48
1.36
1.24
1.12
1.00
REF. N.A.C.A. TR 558, Fig. 18
REYNOLDS NUMBER
1x10^5
2
3
4
5
6
7
8
9
10